# Comprehensive Multiphase NMR Examination of Amino Acids Binding to the Dynamic Shell of Polystyrene Nanoparticles to Understand Environmental Hazards Associated with Nanoscale Plastic

Rajshree Ghosh Biswas<sup>1</sup>, Ronald Soong<sup>1</sup>, Daniel Schmidig<sup>2</sup>, Peter De Castro<sup>2</sup>, Stephan Graf<sup>2</sup>, Falko Busse<sup>3</sup>, André J. Simpson<sup>1\*</sup> and Leah B. Casabianca<sup>4\*</sup>

# **Abstract**

Plastic pollution is a growing environmental concern. In addition to posing hazards to wildlife, micro- and nano-scale plastic particles can adsorb toxic small molecules from polluted waterways, which may be released when these plastic particles are ingested by animals or humans. Previous NMR studies have examined the binding between surface-modified polystyrene nanoparticles and amino acids as models for small molecules with a variety of functional groups. These previous studies, however, could only examine the liquid phase and therefore focused on the small molecules. In the current study, we use comprehensive multiphase NMR (CMP-NMR) to examine both the small molecules and polystyrene nanoparticles in all phases including liquid, solid, and gel-like phase. Through proton spectral editing techniques and <sup>13</sup>C solid-state NMR experiments, we find that the polystyrene nanoparticles contain both a solid and gel-like fraction. The bound amino acid exists primarily in the gel-like phase, with very little amino acid existing in the true solid phase. This suggests that the bound amino acid interacts with the nanoparticle shell rather than the solid-like core. These experiments relied on the ability of CMP-NMR to separately observe the solid, liquid, and gel-like phases of the same sample, and demonstrate the complementary nature of this approach for understanding complex multi-phase systems.

**Keywords:** NMR, nanoparticles, polystyrene, multiphase NMR, plastic, tryptophan, phenylalanine

#### Introduction

Plastic pollution is becoming an important environmental concern. Large plastic pieces present in bodies of water are broken down over time into small pieces, which are further degraded to microand nano-scale particles. Due to their large surface-to-volume ratio, plastic nanoparticles are especially prone to sorption of small molecules that may also be present in polluted waterways. Hastics have been shown to act as a source and sink for toxic small molecules. Understanding how small molecules bind to polystyrene nanoparticles, specifically whether they are sequestered in the core or interact with the flexible groups on the surface, is essential for a full appreciation of the sorption of toxic small molecules from natural water by plastic pollution. This information is also necessary for the design of plastics that intentionally sorb these small molecules for the purpose of environmental remediation.

Amino acids are a nice set of model compounds for small molecules, because they contain a variety of functional groups that are similar to those present in pharmaceuticals, pesticides, and other small molecules that may be of environmental concern. In addition, nano-plastics have been shown to be ingested by filter feeders<sup>7</sup> such as *Daphnia magna*, where strong interactions with

<sup>&</sup>lt;sup>1</sup>Department of Chemistry, University of Toronto Scarborough, Toronto, ON, Canada

<sup>&</sup>lt;sup>2</sup>Bruker BioSpin AG, Industriestrasse 26, 8117 Fällanden, Switzerland

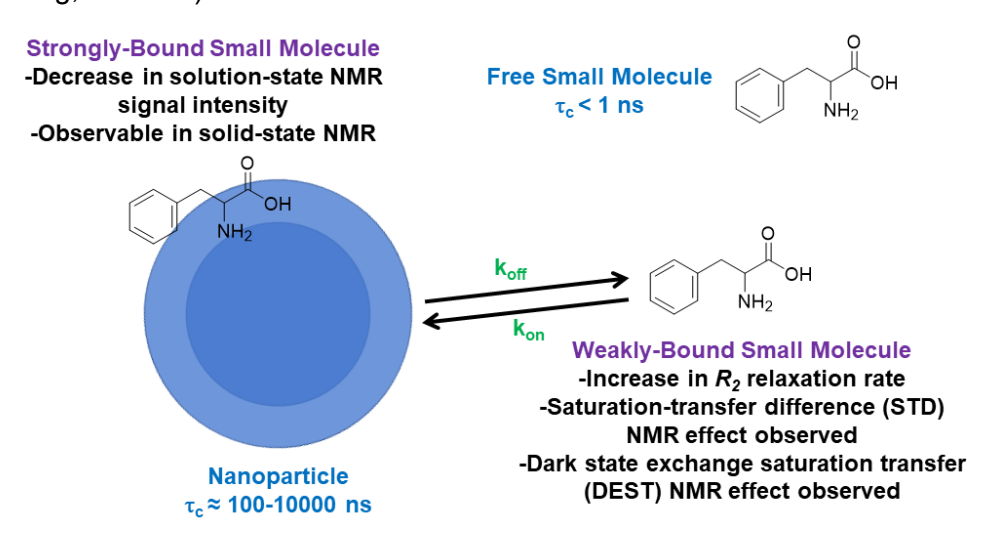
<sup>&</sup>lt;sup>3</sup>Bruker BioSpin GmbH, Rudolf-Plank-Str. 23, 76275 Ettlingen, Germany

<sup>&</sup>lt;sup>4</sup>Department of Chemistry, Clemson University, Clemson, SC, USA

<sup>\*</sup>Corresponding authors: lcasabi@clemson.edu and andre.simpson@utoronto.ca

amino acids as they pass through the digestive tract could reduce availability to the living organisms.

Previous work has shown that amino acids can interact with polystyrene nanoparticles that have been modified with different surface groups. 8,9 The amino acids interact with the modified polystyrene surface through electrostatic interactions, hydrophobic effects, and pi-stacking. Aromatic amino acids tryptophan, phenylalanine, and histidine were especially prone to interactions with the nanoparticles, which may be due to pi-stacking interactions with the styrene groups. Scheme 1 illustrates how strong vs weak binding of small molecules and nanoparticles would be observed in solution-state NMR. Based on this scheme, what we know about the binding between polystyrene nanoparticles and amino acids so far is that weak binding is present, causing an equilibrium between free and bound amino acid. This was evidenced by the observation of STD effects in the presence of nanoparticles and increase in  $R_2$  relaxation rate with subsequent line broadening. However, these experiments relied on observing the small molecule in the liquid phase, so no information was obtained regarding the nanoparticle structure or whether the presence of a small molecule induces a change in the structure of the nanoparticle core or shell. In order to obtain this kind of information, solid-state NMR or gel-phase (High-Resolution Magic Angle Spinning, HRMAS) NMR would be needed.



Scheme 1. Illustration of how strong vs weak binding of ligands to large particles such as nanoparticles manifests in observable NMR effects. Estimates of typical rotational correlation times ( $\tau_c$ ) are taken from references 10 and 11.

Solid-state NMR has been used extensively to characterize nanoparticle-ligand interactions. 12-36 Recently, several novel solution-state NMR methods have been used to gain information on these kinds of interactions as well. 11,37-44 Comprehensive multiphase (CMP) NMR, on the other hand, is the only method that can simultaneously probe solid, liquid, and gel-like phases in an intact sample. 45 A CMP-NMR probe contains the ability to handle the high RF power required for solid-state NMR, as well as a lock, pulse field gradient, and susceptibility matching required for both solution and gel-state NMR. CMP-NMR has been used extensively in environmental studies to monitor structural changes, interactions and follow entire processes: 46 in soil (organization of soil, 47 oil-contamination, 48 biomass-clay interactions, 49 follow contaminants from spill to sequestration 50), plants (13C-labeled seeds, 51 germination and plant growth 52,53), whole organisms (ex vivo 54 and in vivo 55-57) as well as to optimize biofuel extraction, 58 and monitor the effect of biodiesel on commercial rubber. 59 This method is ideal for studying interactions

between small molecules and plastic nanoparticles because the small molecules are freely diffusing in the liquid phase, but the nanoparticles are solid-like in that they are too big to be seen by solution-state NMR, due to undesirable line broadening caused by fast nuclear relaxation. Additionally, CMP-NMR is able to distinguish between gels, semi-solids, and true solids, giving insight into the core and shell behavior of surface-modified polystyrene nanoparticles. Other variations of MAS NMR probes have been developed for *in situ* reaction monitoring, such as the constant-flow MAS probe. These kinds of probes are complementary to the CMP-NMR approach, as they have a large sample volume and flow capabilities, but lack the pulse-field gradient and solid sample handling capabilities of the CMP-NMR probe. Here we use CMP-NMR to examine binding between carboxylate-modified polystyrene nanoparticles (PSNP) and the amino acids phenylalanine (Phe) and tryptophan (Trp), two amino acids that were found previously to bind strongly to PSNPs. The CMP-NMR method allows us to examine not only the core and shell structure of the PSNP, but to determine in which phase the bound amino acid exists.

# Methods

Carboxylate-modified (CML, 40 nm) PSNP were purchased from ThermoFisher Scientific. The nanoparticles were lyophilized prior to use and stored in the freezer. As shown in Figure S1 of the supporting information, TEM images indicate that the nanoparticles retained their spherical morphology after freeze-drying and re-hydration, but were closer to 5-10 nm in diameter. Phenylalanine and tryptophan ("ultrapure", >98.5%) were purchased from BioShop Canada and were used without further purification. Uniformly <sup>13</sup>C, <sup>15</sup>N-labeled phenylalanine was purchased from Silantes (Munich, Germany). Deuterium oxide was from Cambridge Isotope Labs.

For each NMR sample, approximately 10 mg of lyophilized nanoparticles was placed in a 4mm, 50- $\mu$ L zirconia rotor. Phe or Trp was dissolved in  $D_2O$  and this solution was added to the solid in the rotor, and the two were mixed well. The rotor was sealed with a Bruker HR-MAS sealing system.

NMR experiments were run on a 500-MHz Bruker Avance III NMR spectrometer with a commercial <sup>1</sup>H-<sup>13</sup>C-<sup>15</sup>N CMP-NMR probe with both a <sup>2</sup>H lock and a magic angle gradient. The proton 90° pulse was 2.5 μs, spectral width was 20 ppm, acquisition time was 0.8192 seconds, and 128 scans with 8 dummy scans were collected. The recycle delay was adjusted for each sample to be at least 5 times the  $T_1$  of the longest-relaxing peak in the spectrum, and this was 10.82 s for the PSNP-Phe sample and 14.5 s for the PSNP-Trp sample. For carbon crosspolarization (CP) experiments, the total sideband suppression (TOSS) pulse sequence was used. 61,62 8192 scans were collected with 8 dummy scans and a recycle delay of 2s. The spectral width was 301 ppm, acquisition time was 13.5 ms, CP contact time was 1ms, carbon CP power was 20 KHz, and proton CP power was ramped from 35.6 to 71.2 KHz. All experiments were run at 298K and 6666 Hz magic-angle spinning. D<sub>2</sub>O was used as the lock solvent. Exponential line broadening was applied to each spectrum, and the line broadening is listed in the corresponding figure captions. Editing experiments were performed as previously described. 45,58 Briefly, diffusion editing experiments were acquired using a bipolar pulse pair longitudinal encode-decode (BPPLED) sequence. Scans were collected using encoding/decoding gradients of 1.2 ms at ~60 gauss cm<sup>-1</sup> and a diffusion time of 120 ms. CPMG (Carr-Purcell-Meiboom-Gill) filtering was achieved using a total delay of 150 ms with the PROJECT pulse sequence, 63 with the exception of T<sub>2</sub>-filtered CP-MAS which used two echoes (30 µs total echo time) on the proton channel prior to cross-polarization. Inverse diffusion editing (IDE), Relaxation Recovery Arising from Diffusion Editing (RADE) and inverse  $T_2$ -filtered experiments were performed via weighted spectral subtraction as previously described.<sup>45</sup>

### **Results and Discussion**

Figure 1 shows <sup>1</sup>H spectral editing experiments that take advantage of the CMP-NMR method to separately reveal the solution-like, gel-like, and solid-like components in an intact sample. The different phases are separated based on their diffusion coefficients, nuclear relaxation times, and strength of C-H dipolar coupling. Liquids typically diffuse with diffusion coefficients on the order of  $10^{-8}$  m<sup>2</sup>/s, gels move less than  $1\mu m$  during the diffusion delay, and solids move much more slowly with diffusion coefficients less than 10<sup>-11</sup> m<sup>2</sup>/s. <sup>64</sup> Nuclear relaxation times can provide complementary information about molecular motion, but instead of being influenced by the overall dynamics of the molecule, relaxation times report on the local motion of each nucleus. Last, only true, rigid solids will have C-H dipolar coupling that is strong enough to result in cross-polarization in solid-state NMR. For more details readers should refer to the original work by Courtier-Murias in which CMP-NMR and the editing experiments used here were developed and introduced. 45 With <sup>1</sup>H detection, all components except true rigid solids will be detected. True rigid solids that do not swell often have linewidths of many kHz and are not easily detectable by <sup>1</sup>H NMR; as such they are detected through <sup>13</sup>C CP-MAS NMR. Carbon solid-state CP-MAS NMR will be discussed later in the paper. Figure 1 shows spectra of samples containing solid PSNPs that have been rehydrated and mixed with either phenylalanine (PSNP-Phe, Figure 1a-d) or tryptophan (PSNP-Trp. Figure 1e-h). Figure 1 (a,e) are <sup>1</sup>H reference spectra showing signals from all components in <sup>1</sup>H detectable phases (liquids through to semi-solids) of the spectrum. Figure 1 (b,f) are diffusionedited (DE) spectra. In these experiments, a stimulated gradient echo has been applied to selectively refocus only those components of the sample that diffuse slowly (i.e. those that do not physically move positions within the rotor). These spectra contain signals from the gel-like components of the sample and are dominated by PSNP signals. On the other hand, Figure 1 (c, g) are inverse diffusion-edited (IDE) spectra, which show signal only from components in the liquid phase (with diffusion coefficients ~10<sup>-8</sup> m<sup>2</sup>/s). Construction of the IDE spectra is shown in detail in Figure 2 (a-c). The IDE spectrum is constructed by subtracting the DE spectrum (delays and gradient turned on) from a reference spectrum with delays on but gradients off, selecting only signals that diffuse quickly and relax slowly. Last, Figure 1 (d,h) are  $T_2$ -filtered experiments showing only those components that have long transverse relaxation times (>30 ms), specifically liquids and flexible regions of solids and gels. Interestingly, diffusion-based editing selects based on the entire molecule whereas relaxation-based editing is also influenced by local dynamics within a molecule. As such, signals that appear in (d,h) but not in (c,q) are likely from dynamic regions of larger molecules. For the samples in Figure 1, this is mainly the dynamic coating on the outside of the nanoparticles.

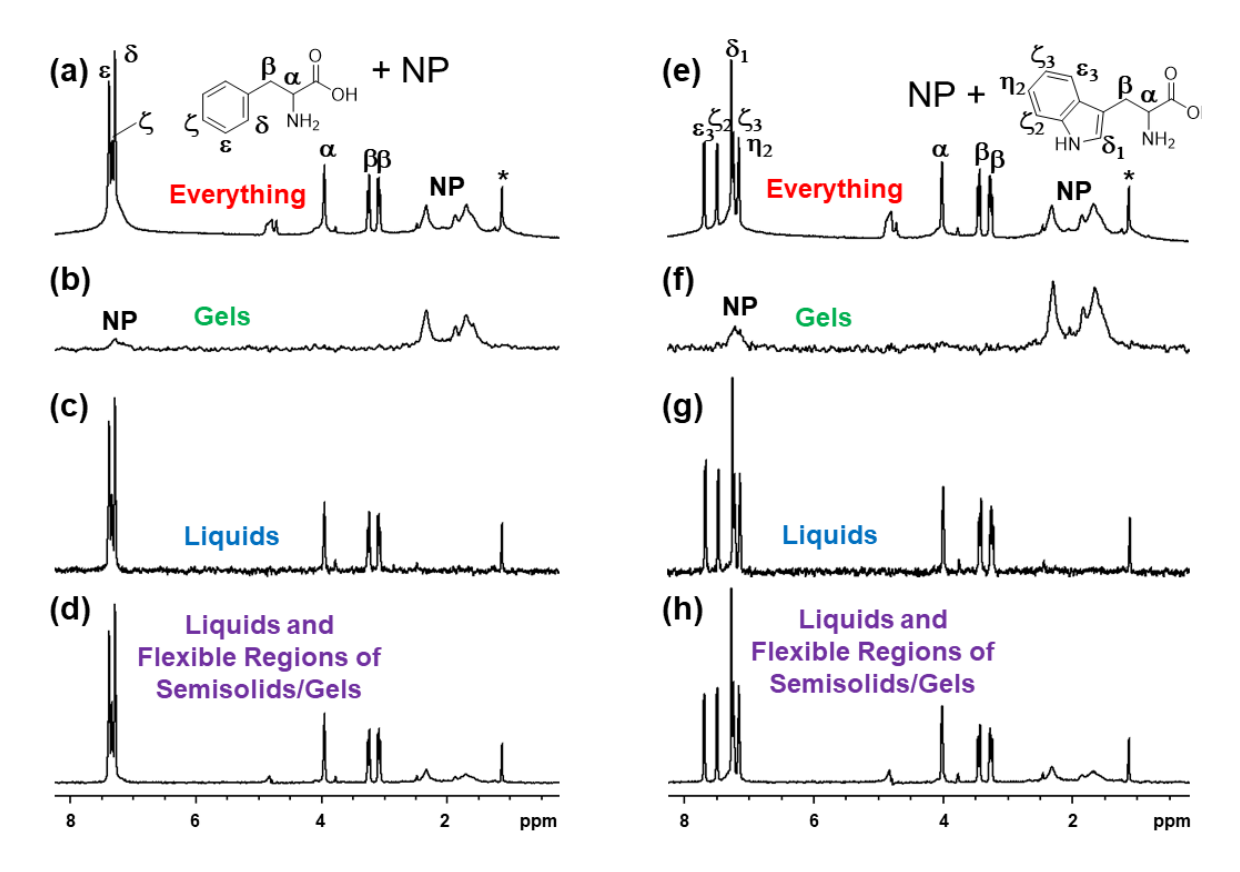


**Figure 1.** <sup>1</sup>H CMP-NMR spectral editing experiments. (a-d) PSNP-Phe, (e-h) PSNP-Trp (a,e) Reference spectra containing signals from all phases (delays off, gradients off) (b, f) diffusion edited spectra (delays on, gradients on) showing signals from slowly-diffusing components, i.e. gels (c, g) inverse diffusion edited spectra showing signals from fast-diffusing species, i.e. liquids only, and (d,h)  $T_2$ -filtered spectrum showing signals from slowly-relaxing species, i.e. liquids and flexible regions of solids, semi-solids, and gels. Line broadening applied was 10 Hz in (b,f) and 3 Hz in all others. The vertical scales are arbitrary. The (\*) indicates signals from trace isopropanol impurity in the sample. The residual signal from suppressed water is present at 4.7 ppm. NP = nanoparticle.

The reference spectra in Figure 1 (a,e) show signals from both the polystyrene nanoparticle and the amino acid. The polystyrene nanoparticle signals are generally broader, as expected for these larger, solid-like particles. Indeed, these signals are emphasized in the DE spectra in Figure 1(b,f). Note that there is some overlap in the aromatic region between the styrene groups of the PSNP and the aromatic amino acid peaks in the reference spectra, leading to a broad PSNP peak superimposed on the sharp amino acid peaks. These two components are nicely resolved in the subsequent spectral editing experiments shown in Figure 1 (b,f) and (c,g). The PSNP nanoparticle peaks appear in the DE spectra (b,f), which select gel-like components and the amino acid peaks appear in the IDE spectra in (c,g), which select liquid-like signals. The  $T_2$ -filtered experiments in Figure 1 (d,h) also contain peaks from both the amino acids and nanoparticle. The amino acids are in the liquid phase, so they would be expected to have long  $T_2$  relaxation times, but the presence of the PSNP peaks in this spectrum indicates that these PSNP regions contain additional flexibility that affords additional molecular motion, attenuating the dipolar interactions. Since dipolar interactions lead to enhanced relaxation, when these interactions are reduced by molecular motion, relaxation of these nuclei is slowed. These regions could be the flexible linkers

of the surface-modified groups. The commercial PSNPs we purchased have proprietary groups on the surface containing a carboxylate group, but we postulate that these groups may also contain an aliphatic linker that connects the carboxylate group to the PSNP core.

The amino acids phenylalanine and tryptophan have been previously shown to bind to PSNPs. Saturation-transfer difference (STD) NMR experiments indicate that the bound amino acids are in equilibrium with free amino acids in the liquid state. The bound amino acids could be interacting with the flexible linker or PSNP shell, or they could be binding to the nanoparticle core as true solids. In order to resolve these two possibilities, we rely on relaxation recovery arising from diffusion editing (RADE)<sup>45</sup> and cross-polarization (CP) experiments.

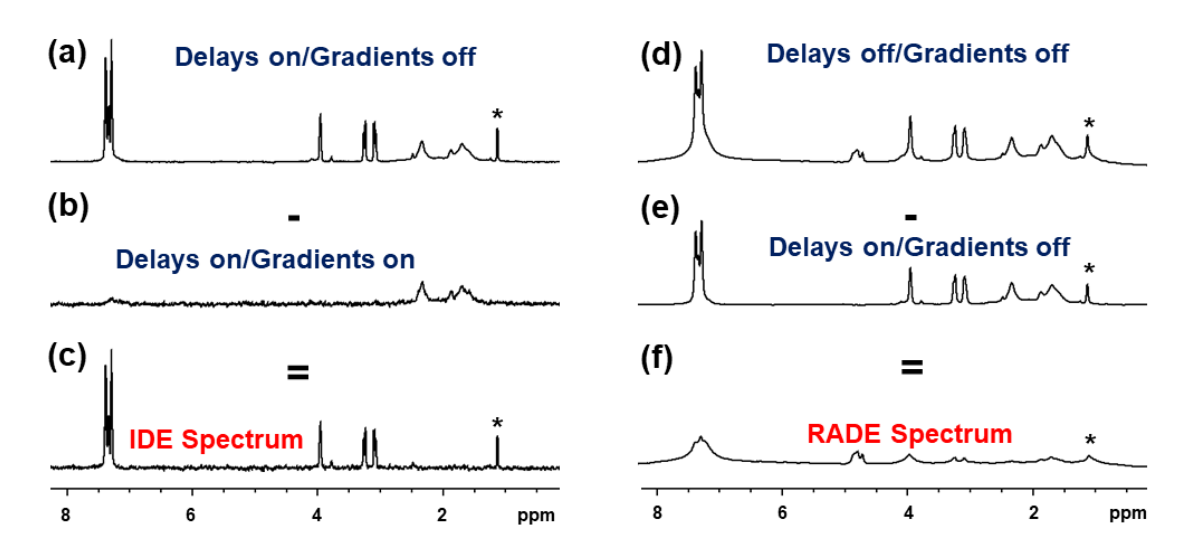


**Figure 2.** Details of spectral editing subtraction, using PSNP-Phe as an example. The IDE spectrum (c) is formed by subtracting the diffusion edited spectrum where both diffusion delays and gradients are turned on (b) from the spectrum with delays on but gradients off (a). Line broadening of 3 Hz is used to emphasize the liquid components in the IDE spectrum. The RADE spectrum (f) is formed by subtracting the spectrum with delays on but gradients off (e) from the reference spectrum where both delay and gradients are off (d). (e) is the same as (a) but the line broadening here is 10 Hz in order to emphasize the gel-like components in the RADE spectrum. The (\*) indicates signals from trace isopropanol impurity in the sample.

Construction of the RADE spectra is shown in Figure 2 (d-f). The RADE spectrum accounts for relaxation that can occur during the diffusion delays when diffusion-based-editing is used. It contains signals from rigid gels and semi-solids that may be relaxing too quickly to be seen in the diffusion edited spectrum in Figure 1 (b and f). The RADE spectrum is constructed by subtracting signals from an experiment with delays on but gradients off (the same experiment used to construct the IDE spectrum) from the reference spectrum with both gradients and delays off. This is a critical experiment as it selects signals from gels that relax during the diffusion editing experiment that could be missed if diffusion editing is used alone. Semi-solid/gel-like components that relax quickly will dephase during the DE experiment and will not be observed. The RADE spectrum recovers these signals. Thus, gel-like components may appear in either the DE spectrum and/or the RADE spectrum, so both spectra need to be considered to account for all gel-like/semi-solid components in a sample.

The RADE spectra for PSNP-Phe and PSNP-Trp are shown in Figure 3. These spectra indicate that there is some amino acid in each case that is present in the semi-solid or rigid gel-like phase.

Expanded portions of the RADE spectra are shown in Figure 4 and are compared to the IDE (liquid-like) spectrum of each sample. This comparison indicates that the chemical shifts of peaks appearing in the RADE spectra correspond to those of the amino acids, rather than the polystyrene nanoparticles. Some cancellation artifacts are also visible in these spectra at the position of the sharp signals from the amino acids in the liquid phase. These residual peaks are due to imperfect subtraction of the two spectra in constructing the RADE difference spectrum. The presence of broad amino acid peaks in the RADE spectra indicates that the bound amino acid in each case is interacting with the flexible, semi-solid region of the PSNP shell instead of the solid-like PSNP core, and is in a gel-like rather than true crystalline solid form. Note that these amino acid peaks are not visible in the DE spectra, so without the RADE experiment, these signals would have been missed. This emphasizes the importance of collecting a RADE spectrum in addition to a DE spectrum in order to observe all gel signals, including those that relax quickly. Asterisks in the spectra indicate the presence of isopropanol impurity in the sample. Interestingly, isopropanol was also previously shown<sup>65</sup> to interact with the surface of these PSNPs. There is a peak corresponding to the chemical shift of isopropanol in the RADE spectrum as well, which is consistent with a small fraction of isopropanol becoming entrapped in the coating and thus appearing as a "gel".

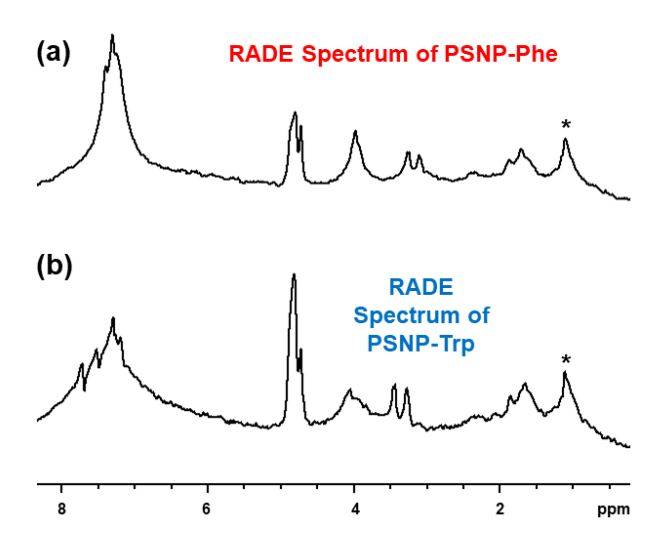


**Figure 3.** <sup>1</sup>H RADE spectra of (a) NP-Phe and (b) NP-Trp. Line broadening was 10 Hz in both cases.

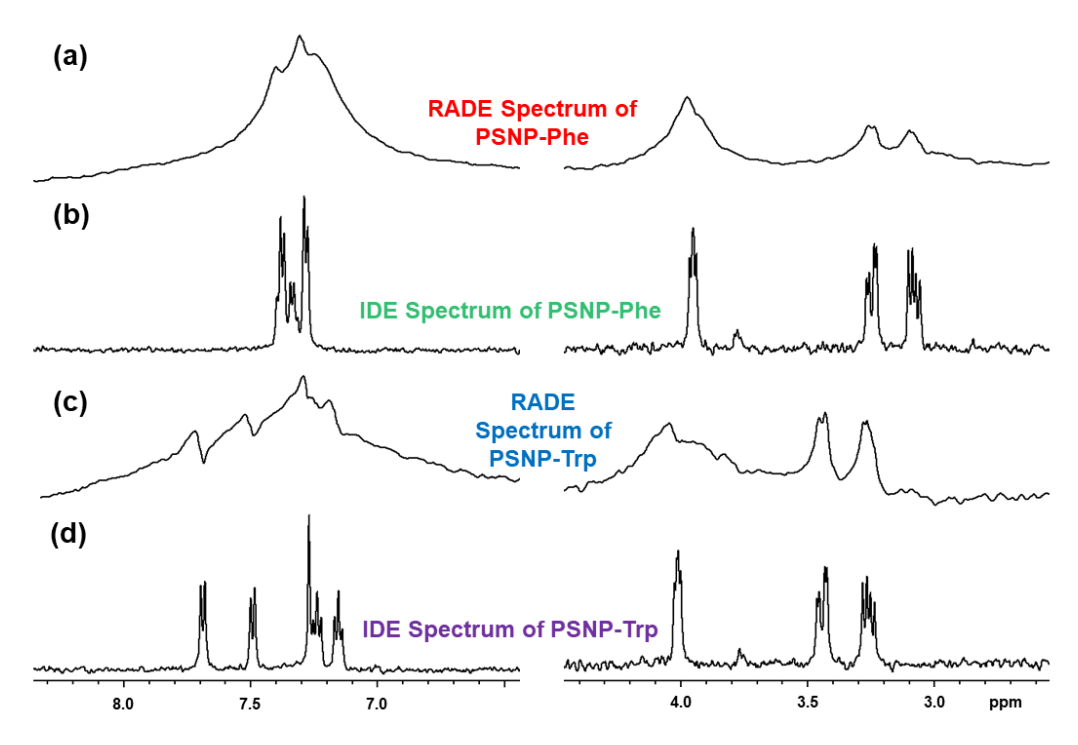


*Figure 4.* Portions of the <sup>1</sup>H (a) RADE spectrum of PSNP-Phe (b) IDE spectrum of PSNP-Phe (c) RADE spectrum of PSNP-Trp (d) IDE spectrum of PSNP-Trp

Last, we capitalized on the advantage of CMP-NMR to detect true solids via carbon cross-polarization experiments on the same samples. This can only be done with a CMP probe, because it is the only probe that has not only the ability to spin at the magic angle, a lock, and a gradient channel (for liquids and gels) but is also capable of producing high-power proton pulses (100 kHz) allowing true crystalline solids to be observed as well (solids). Note that traditional HR-MAS probes cannot handle high-power solids experiments involving CP or high-power decoupling and this should never be attempted as it would lead to severe probe damage. CMP-NMR probes have been specifically redesigned to handle the high power requirements for solid-state NMR.

Carbon CP spectra are shown in Figure 5 (a-b) for the PSNP-Phe and PSNP-Trp samples. When scaled to adjust for slightly different amounts of solid in each sample, these spectra look identical to within the noise level, and are also identical to the CP spectrum of PSNP that was re-hydrated with pure  $D_2O$  (Figure 5c). These signals are relatively weak as at natural abundance only 1 in every 100 carbons is  $^{13}C$ . The CP spectra for all three samples, however, clearly show peaks from the PSNP nanoparticles. CP spectra only show signals from rigid solids, so at least part of the PSNP core exists in true solid form. No signals from the amino acids are visible in these spectra because the amount of amino acid existing in the true solid form is so low that this, coupled with the low natural abundance of  $^{13}C$ , is causing these signals to be below the detection limit, even with the signal-enhancing effect of cross-polarization.

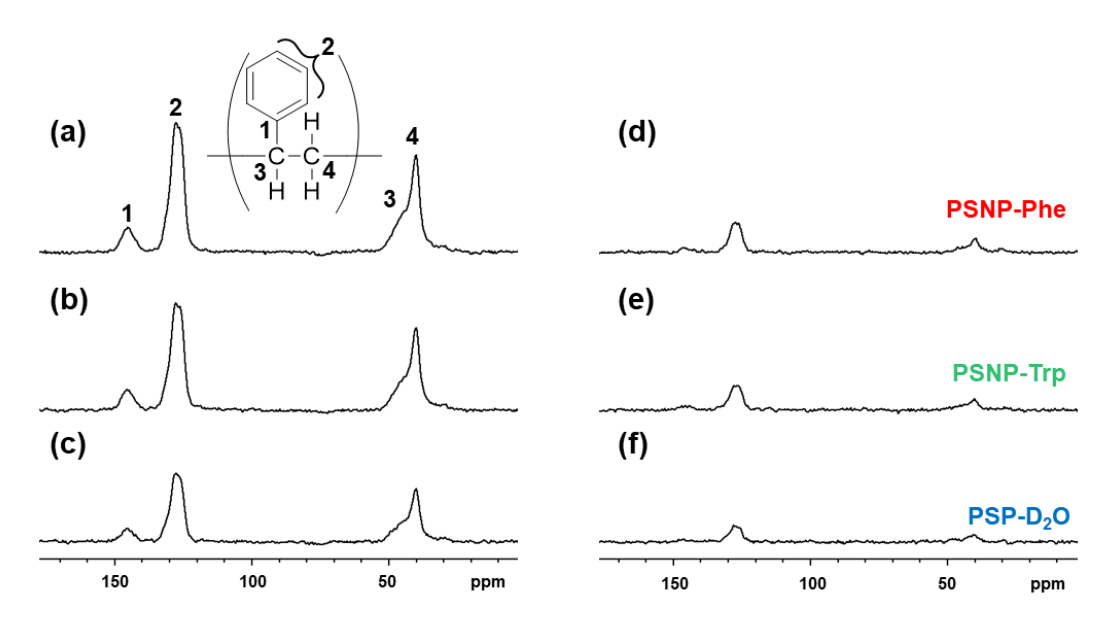


**Figure 5.** CP spectra for (a,d) PSNP-Phe and (b,e) PSNP-Trp (c,f) PSNP-D<sub>2</sub>O (a-c) CP-TOSS, (d-f)  $T_2$ -filtered CP-TOSS. Line broadening was 50 Hz in each case.

The  $T_2$ -filtered CP spectra are shown in Figure 5 (d-f) for PSNP-Phe, PSNP-Trp, and PSNP-D<sub>2</sub>O. As with the CP spectra, when scaled to adjust for different amounts of solid in each sample, these spectra are again identical to within the noise level. The  $T_2$ -filtered CP experiments select only the more dynamic solids (amorphous solids and/or semi-solids) that have longer  $T_2$  relaxation times (>10  $\mu$ s), compared to quickly-relaxing rigid solids. The  $T_2$ -filtered CP spectra for PSNP-Phe and PSNP-Trp have the same profile as the full CP spectra, but reduced intensity. This indicates that all carbons giving rise to observable polystyrene peaks have an equal fraction in the rigid solid and flexible gel-like phase.

In order to further investigate if any amino acid signal could be seen in the solid state, we prepared a sample using uniformly <sup>13</sup>C-labeled phenylalanine. These spectra are shown in Figure 6. Here, signals from the <sup>13</sup>C-labeled phenylalanine are clearly visible. CP experiments are generally only semi-quantitative, but if we assume that the signals corresponding to Phe and PSNP are of roughly equal intensity in these spectra, since PSNP is still at natural abundance, it means that there is roughly 1 <sup>13</sup>C-Phe molecule in the true solid phase for every 100 PSNP carbons in the true solid phase. Thus, we can conclude that very little of the bound Phe is in the true solid, while most of it is a semisolid or rigid gel. This indicates that most of the bound Phe is interacting with the flexible, linker regions of the PSNP shell rather than the solid-like PSNP core.

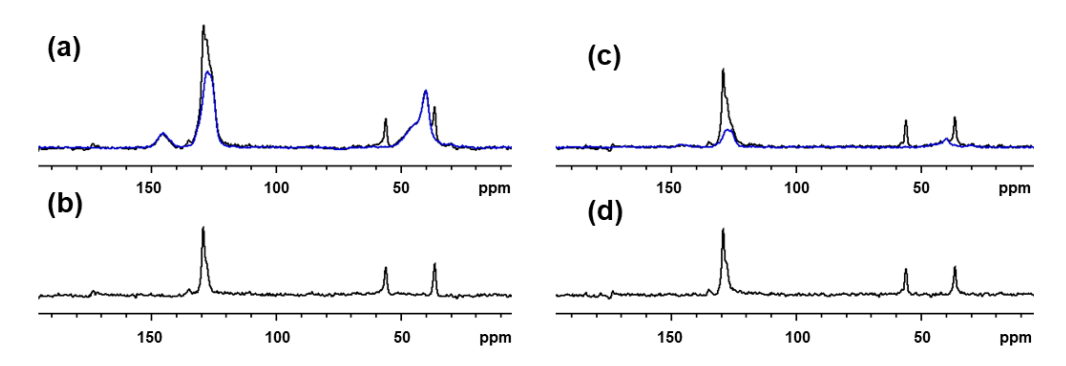


**Figure 6.** Carbon CP spectra of PSNP-Phe samples with natural abundance and  $^{13}$ C-labeled phenylalanine. (a) blue: NP-Phe, black: NP- $^{13}$ C labeled Phe (scaled by 0.6573 to reflect the slightly different amounts of solid in each sample) (b) difference spectrum black-blue from (a) showing only peaks from  $^{13}$ C phenylalanine (c) same as (a) but CP- $^{7}$ 2 filtered experiment, showing only peaks with long  $^{7}$ 2 relaxation times (d) difference black-blue from (c). Line broadening was 50 Hz in each case.

 $T_2$ -filtered CP experiments shown in Figure 6 (c-d) also indicate that the bound polystyrene is in the semi-solid/rigid-gel like phase rather than true solid phase. Whereas the signal from polystyrene is attenuated in the presence of the  $T_2$ -filter, the phenylalanine peaks are the same intensity in the CP and  $T_2$ -filtered CP experiments. (Compare Figure 6b and d). Thus, these experiments indicate that most of the  $^{13}$ C-labeled phenylalanine carbon is in a solid phase that exhibits dynamics (for example semi-solids or rigid-gel). The carbon CP experiments were only possible due to the  $^{13}$ C-labeled phenylalanine and would be prohibitively expensive to carry out on a regular basis. However, with the advancement of CMP probes and experiments that have been optimized for carbon detection,  $^{66}$  we expect that these kinds of experiments will be possible on natural-abundance samples in the near future.

# **Conclusions**

Comprehensive multiphase NMR has been used to examine the interactions between amino acids phenylalanine and tryptophan and polystyrene nanoparticles by allowing the observation of all phases (liquids, gels, and solids) in the same sample. Whereas previous studies have relied on measuring the free amino acid in the liquid state, results of the current study indicate that the bound amino acids are interacting with the flexible gel-like shell of the polystyrene nanoparticle rather than being sequestered in the true solid-like core.

Using spectral editing experiments, signals from polystyrene were found to be in the gel-like phase, but signals from polystyrene also appear in  $T_2$ -filtered experiments, indicating that these signals come from flexible regions of gels. Carbon CP experiments also indicate that some of the polystyrene exists in true solid form.

Amino acid peaks dominate the IDE spectra, which select only fast-diffusing, liquid-like samples. However, RADE experiments also show signals from amino acids, indicating that the bound amino acid signal is in a gel-like or semi-solid state. The CP experiments with natural abundance and <sup>13</sup>C-labeled phenylalanine also confirm that very little of the bound polystyrene exists as a true solid. Therefore, we can conclude that there are portions of the polystyrene nanoparticle that are true solids as well as other portions that are flexible semi-solids or gels. The bound amino acids phenylalanine and tryptophan are primarily in the gel-like or semisolid phase, indicating that they interact with the flexible shell of the PSNP rather than the solid-like PSNP core.

These experiments showcase the unique advantages of the CMP-NMR approach. Due to the specialized CMP-NMR probe, we were able to selectively examine the liquid-like, gel-like and true solid phases of these samples. The RADE experiment allowed us to recover signals from bound amino acids, which were missed in the diffusion-edited spectra due to fast relaxation. Collecting the true solid phase carbon spectra was also instrumental to concluding that very little of the bound amino acid is present as a true solid. As such, CMP-NMR holds great potential to observe interactions in samples with minimal sample preparation. This may be used to understand real-world applications of metabolite binding to the ever-growing presence of micro/nano-plastics in the environment.

# **Supplemental Information**

Transmission electron microscopy images of the polystyrene nanoparticles before and after freeze-drying.

# **Acknowledgements**

LBC acknowledges support from the US National Science Foundation (grant number CHE-1751529). AJS would like to thank the Natural Sciences and Engineering Research Council of Canada (NSERC) [Alliance (ALLRP 549399), Alliance (ALLRP 555452) and Discovery Programs (RGPIN-2019-04165)], the Centre national de la recherche scientifique (CNRS) PhD Mobility Funding Programme, the Canada Foundation for Innovation (CFI), the Ontario Ministry of Research and Innovation (MRI), and the Krembil Foundation for providing funding. We thank Dr. Eric Formo of the Georgia Electron Microscopy Lab, University of Georgia, for the electron microscopy images.

## **Conflict of Interest Statement**

The Bruker scientists on the paper built and designed the probe as part of a collaboration, but had no input into the experimental design, results or interpretation of the study.

#### References

- 1. Andrady, A. L. The Plastic in Microplastics: A Review, Mar. Pollut. Bull. 2017, 119, 12-22.
- 2. Andrady, A. L. Microplastics in the Marine Environment. *Mar. Pollut. Bull.* **2011**, 62, 1596-1605.
- 3. Fred-Ahmadu, O. H.; Bhagwat, G.; Oluyoye, I.; Benson, N. U.; Ayejuyo, O. O.; Palanisami, T. Interaction of chemical contaminants with microplastics: Principles and perspectives, *Sci. Total. Environ.* **2000**, *706*, 135978.
- 4. Rochman, C. M.; Hoh, E.; Hentschel, B. T.; Kaye, S. Long-term field measurement of sorption of organic contaminants to five types of plastic pellets: implications for plastic marine debris. *Environ. Sci. Technol.* **2013**, 47, 1646–1654.
- 5. Rochman, C. M.; Manzano, C.; Hentschel, B. T.; Simonich, S. L. M.; Hoh, E. Polystyrene plastic: a source and sink for polycyclic aromatic hydrocarbons in the marine environment. *Environ. Sci. Technol.* **2013**, *47*, 13976–13984.

- 6. Zare, E. N.; Fallah, Z.; Le, V. T.; Doan, V.-D.; Mudhoo, A.; Joo, S.-W.; Vasseghian, Y.; Tajbakhsh, M.; Moradi, O.; Sillanpää, M.; Varma, R. S. Remediation of pharmaceuticals from contaminated water by molecularly imprinted polymers: a review, *Environ. Chem. Lett.* **2022**.
- 7. Dutta Majumdar, R.; Akhter, M.; Fortier-McGill, B.; Soong, R.; Liaghati-Mobarhan, Y.; Simpson, A. J.; Spraul, M.; Schmidt, S.; Heumann, H. In Vivo Solution-State NMR-Based Environmental Metabolomics, *eMagRes* **2017**, *6*, 133-148.
- 8. Zhang, Y.; Casabianca, L. B. Probing Amino Acid Interaction with a Polystyrene Nanoparticle Surface Using Saturation-Transfer Difference (STD)-NMR, *J. Phys. Chem. Lett.* **2018**, 9, 6921-6925.
- 9. Xu, H.; Casabianca, L. B. Probing Driving Forces for Binding Between Nanoparticles and Amino Acids by Saturation-Transfer Difference NMR, *Sci. Rep.* **2020**, *10*, 12351.
- 10. Curto, E. V.; Moseley, H. N. B.; Krishna, N. R. CORCEMA evaluation of the potential role of intermolecular transferred NOESY in the characterization of ligand-receptor complexes, *J. Comput. Aid. Mol. Des.* **1996**, *10*, 361-371.
- 11. Perera, Y. R.; Hill, R. A.; Fitzkee, N. C. Protein Interactions with Nanoparticle Surfaces: Highlighting Solution NMR Techniques, *Isr. J. Chem.* **2019**, *59*, 962-979.
- 12. Guo, C.; Jordan, J. S.; Yarger, J. L.; Holland, G. P. Highly Efficient Fumed Silica Nanoparticles for Peptide Bond Formation: Converting Alanine to Alanine Anhydride, *ACS Appl. Mater. Interfaces* **2017**, *9*, 17653-17661.
- 13. Guo, C.; Holland, G. P. Alanine Adsorption and Thermal Condensation at the Interface of Fumed Silica Nanoparticles: A Solid-State NMR Investigation, *J. Phys. Chem. C* **2015**, *119*, 25663-25672.
- 14. Guo, C.; Holland, G. P. Investigating Lysine Adsorption on Fumed Silica Nanoparticles, *J. Phys. Chem. C* **2014**, *118*, 25792-25801.
- 15. Marchetti, A.; Chen, J.; Pang, Z.; Li, S.; Ling, D.; Deng, F.; Kong, X. Understanding Surface and Interfacial Chemistry in Functional Nanomaterials via Solid-State NMR, *Adv. Mater.* **2017**, 29, 1605895.
- 16. Lee, D.; Kaushik, M.; Coustel, R.; Chenavier, Y.; Chanal, M.; Bardet, M.; Dubois, L.; Okuno, H.; Rochat, N.; Duclairoir, F.; Mouesca, J.-M.; De Paepe, G. Solid-State NMR and DFT Combined for the Surface Study of Functionalized Silicon Nanoparticles, *Chem. Eur. J.* **2015**, 21. 16047-16058.
- 17. Karki I.; Wang, H.; Geise, N. R.; Wilson, B. W.; Lewis, J. P.; Gullion, T. Tripeptides on Gold Nanoparticles: Structural Differences between Two Reverse Sequences as Determined by Solid-State NMR and DFT Calculations, *J. Phys. Chem. B* **2015**, *119*, 11998-12006.
- 18. Cui, J. L.; Chatterjee, P.; Slowing, I. I.; Kobayashi, T. In Situ Si-29 solid-state NMR study of grafting of organoalkoxysilanes to mesoporous silica nanoparticles, *Micropor. Mesopor. Mat.* **2022**, 339, 112019.
- 19. Rothermel, N.; Limbach, H. H.; del Rosal, I.; Ponteu, R.; Mencia, G.; Chaudret, B.; Buntkowsky, G.; Gutmann, T. In Situ Si-29 solid-state NMR study of grafting of organoalkoxysilanes to mesoporous silica nanoparticles, *Catal. Sci. Technol.* **2021**, *11*, 4509-4520.
- 20. Li, X.; Porcino, M.; Qiu, J. W.; Constantin, D.; Martineau-Corcos, C.; Gref, R. Doxorubicin-Loaded Metal-Organic Frameworks Nanoparticles with Engineered Cyclodextrin Coatings: Insights on Drug Location by Solid State NMR Spectroscopy, *Nanomaterials* **2021**, *11*, 945.

- 21. Porcino, M.; Li, X.; Gref, R.; Martineau-Corcos, C. Solid-state NMR spectroscopy as a powerful tool to investigate the location of fluorinated lipids in highly porous hybrid organic-inorganic nanoparticles, *Magn. Reson. Chem.* **2021**, *59*, 1038-1047.
- 22. Lau, S.; Stanhope, N.; Griffin, J.; Hughes, E.; Middleton, D. A. Drug orientations within statin-loaded lipoprotein nanoparticles by F-19 solid-state NMR, *Chem. Commun.* **2019**, *55*, 13287-13290.
- 23. Klimavicius, V.; Neumann, S.; Kunz, S.; Gutmann, T.; Buntkowsky, G. Room temperature CO oxidation catalysed by supported Pt nanoparticles revealed by solid-state NMR and DNP spectroscopy, *Catal. Sci. Technol.* **2019**, *9*, 3743-3752.
- 24. Roohnikan, M.; Permack, K. C.; Guzman-Juarez, B.; Toader, V.; Rey, A.; Reven, L. Hydrogen-bonded LC nanocomposites: characterisation of nanoparticle-LC interactions by solid-state NMR and FTIR spectroscopies, *Liq. Cryst.* **2019**, *46*, 1067-1078.
- 25. Rothermel, N.; Rother, T.; Ayvali, T.; Martinez-Prieto, L. M.; Philippot, K.; Limbach, H. H.; Chaudret, B.; Gutmann, T.; Buntkowsky, G. Reactions of D-2 with 1,4-Bis(diphenylphosphino) butane-Stabilized Metal Nanoparticles-A Combined Gas-phase NMR, GC-MS and Solid-state NMR Study, *ChemCatChem* **2019**, *11*, 1465-1471.
- 26. Kobayashi, T.; Singappuli-Arachchige, D.; Slowing, I. I.; Pruski, M. Spatial distribution of organic functional groups supported on mesoporous silica nanoparticles (2): a study by H-1 triple-quantum fast-MAS solid-state NMR, *Phys. Chem. Chem. Phys.* **2018**, *20*, 22203-22209.
- 27. Spataro, G.; Champouret, Y.; Florian, P.; Coppel, Y.; Kahn, M. L. Multinuclear solid-state NMR study: a powerful tool for understanding the structure of ZnO hybrid nanoparticles, *Phys. Chem. Chem. Phys.* **2018**, *20*, 12413-12421.
- 28. Kobayashi, T.; Singappuli-Arachchige, D.; Wang, Z. R.; Slowing, I. I.; Pruski, M. Spatial distribution of organic functional groups supported on mesoporous silica nanoparticles: a study by conventional and DNP-enhanced Si-29 solid-state NMR, *Phys. Chem. Chem. Phys.* **2017**, *19*, 1781-1789.
- 29. Davidowski, S. K.; Holland, G. P. Solid-State NMR Characterization of Mixed Phosphonic Acid Ligand Binding and Organization on Silica Nanoparticles, *Langmuir* **2016**, *32*, 3253-3261.
- 30. Guo, C. C.; Holland, G. P.; Yarger, J. L. Lysine-Capped Silica Nanoparticles: A Solid-State NMR Spectroscopy Study, *MRS Advances* **2016**, *1*, 2261-2266.
- 31. Davidowski, S. K.; Lisowski, C. E.; Yarger, J. L. Characterizing mixed phosphonic acid ligand capping on CdSe/ZnS quantum dots using ligand exchange and NMR spectroscopy, *Magn. Reson. Chem.* **2016**, *54*, 234-238.
- 32. Wang, F. F.; Zhang, R. C.; Wu, Q.; Chen, T. H.; Sun, P. C.; Shi, A. C. Probing the Nanostructure, Interfacial Interaction, and Dynamics of Chitosan-Based Nanoparticles by Multiscale Solid-State NMR, *ACS Appl. Mater. Inter.* **2014**, *6*, 21397-21407.
- 33. Lee, D.; Monin, G.; Doung, N. T.; Lopez, I. Z.; Bardet, M.; Mareau, V.; Gonon, L.; De Paepe, G. Untangling the Condensation Network of Organosiloxanes on Nanoparticles using 2D Si-29-Si-29 Solid-State NMR Enhanced by Dynamic Nuclear Polarization, *J. Am. Chem. Soc.* **2014**, *136*, 13781-13788.
- 34. Neouze, M.-A.; Kronstein, M.; Litschauer, M.; Puchberger, M.; Coelho, C.; Bonhomme, C.; Gervais, C.; Tielens, F. Exploring the Molecular Structure of Imidazolium-Silica-Based Nanoparticle Networks by Combining Solid-State NMR Spectroscopy and First-Principles Calculations, *Chem. Eur. J.* **2014**, *20*, 15188-15196.

- 35. Faulkner, R. A.; DiVerdi, J. A.; Yang, Y.; Kobayashi, T.; Maciel, G. E. The Surface of Nanoparticle Silicon as Studied by Solid-State NMR, *Materials* **2013**, *6*, 18-46.
- 36. Arnold, A. A.; Terskikh, V.; Li, Q. Y.; Naccache, R.; Marcotte, I.; Capobianco, J. A. Structure of NaYF4 Upconverting Nanoparticles: A Multinuclear Solid-State NMR and DFT Computational Study, *J. Phys. Chem. C* **2013**, *117*, 25733-25741.
- 37. An, Y.; Sedinkin, S. L.; Venditti, V. Solution NMR methods for structural and thermodynamic investigation of nanoparticle adsorption equilibria, *Nanoscale Adv.* **2022**, *4*, 2583-2607.
- 38. Xiang, X. Y.; Hansen, A. L.; Yu, L.; Jameson, G.; Bruschweiler-Li, L.; Yuan, C. H.; Bruschweiler, R. Observation of Sub-Microsecond Protein Methyl-Side Chain Dynamics by Nanoparticle-Assisted NMR Spin Relaxation, *J. Am. Chem. Soc.* **2021**, *143*, 13593-13604.
- 39. Xu, J. X.; Alom, M. S.; Fitzkee, N. C. Quantitative Measurement of Multiprotein Nanoparticle Interactions Using NMR Spectroscopy, *Anal. Chem.* **2021**, *93*, 11982-11990.
- 40. Xue, M. J.; Sampath, J.; Gebhart, R. N.; Haugen, H. J.; Lyngstadaas, S. P.; Pfaendtner, J.; Drobney, G. Studies of Dynamic Binding of Amino Acids to TiO2 Nanoparticle Surfaces by Solution NMR and Molecular Dynamics Simulations, *Langmuir* **2020**, *36*, 10341-10350.
- 41. Assfalg, M.; Ragona, L.; Pagano, K.; D'Onofrio, M.; Zanzoni, S.; Tomaselli, S.; Molinari, H. The study of transient protein-nanoparticle interactions by solution NMR spectroscopy, *BBA-Proteins*. *Proteom*. **2016**, *1864*, 102-114.
- 42. Wardenfelt, S.; Xiang, X. Y.; Xie, M. Z.; Yu, L.; Bruschweiler-Li, L.; Bruschweiler, R. Broadband Dynamics of Ubiquitin by Anionic and Cationic Nanoparticle Assisted NMR Spin Relaxation, *Angew. Chem. Int. Ed.* **2021**, *60*, 148-152.
- 43. Xie, M. Z.; Yu, L.; Bruschweiler-Li, L.; Xiang, X. Y.; Hansen, A. L.; Bruschweiler, R. Functional protein dynamics on uncharted time scales detected by nanoparticle-assisted NMR spin relaxation, *Sci. Adv.* **2019**, *5*, eaax5560.
- 44. Ceccon, A.; Tugarinov, V.; Bad, A.; Clore, G. M. Global Dynamics and Exchange Kinetics of a Protein on the Surface of Nanoparticles Revealed by Relaxation-Based Solution NMR Spectroscopy, *J. Am. Chem. Soc.* **2016**, *138*, 5789-5792.
- 45. Courtier-Murias, D.; Farooq, H.; Masoom, H.; Botana, A.; Soong, R.; Longstaffe, J. G.; Simpson, M. J.; Maas, W. E.; Fey, M.; Andrew, B.; Struppe, J.; Hutchins, H.; Krishnamurthy, S.; Kumar, R.; Monette, M.; Stronks, H. J.; Hume, A.; Simpson, A. J. Comprehensive multiphase NMR spectroscopy: Basic experimental approaches to differentiate phases in heterogeneous samples, *J. Magn. Reson.* **2012**, *217*, 61-67.
- 46. Simpson, A. J.; Courtier-Murias, D.; Longstaffe, J. G.; Masoom, H.; Soong, R.; Lam, L.; Sutrisno, A.; Farooq, H.; Simpson, M. J.; Maas, W. E.; Fey, M.; Andrew, B.; Struppe, J.; Hutchins, H.; Krishnamurthy, S.; Kumar, R.; Monette, M.; Stronks, H. J. Environmental Comprehensive Multiphase NMR, *eMagRes*, **2013**, *2*, 399-414.
- 47. Masoom, H.; Courtier-Murias, D.; Farooq, H.; Soong, R.; Kelleher, B. P.; Zhang, C.; Maas, W. E.; Fey, M.; Kumar, R.; Monette, M.; Stronks, H. J.; Simpson, M. J.; Simpson, A. J. Soil Organic Matter in Its Native State: Unravelling the Most Complex Biomaterial on Earth, *Environ. Sci. Technol.* **2016**, *50*, 1670-1680.
- 48. Farooq ,H.; Courtier-Murias, D.; Simpson, M. J.; Maas, W. E.; Fey, M.; Andrew, B.; Struppe, J.; Hutchins, H.; Krishnamurthy, S.; Kumar, R.; Monette, M.; Stronks, H. J.; Simpson, A. J. Characterization of oil contaminated soils by comprehensive multiphase NMR, *Environ. Chem.* **2015**, *12*, 227-235.

- 49. Olivelli, M. S.; Fugariu, I.; Torres Sánchez, R. M.; Curutchet, G.; Simpson, A. J.; Simpson, M. J. Unraveling Mechanisms behind Biomass–Clay Interactions Using Comprehensive Multiphase Nuclear Magnetic Resonance (NMR) Spectroscopy, *ACS Earth Space Chem.* **2020**, *4*, 2061-2072.
- 50. Masoom, H.; Courtier-Murias, D.; Soong, R.; Maas, W. E.; Fey, M.; Kumar, R.; Monette, M.; Stronks, H. J.; Simpson, M. J.; Simpson, A. J. From Spill to Sequestration: The Molecular Journey of Contamination via Comprehensive Multiphase NMR, *Env. Sci. Technol.* **2015**, *49*, 13983-13991.
- 51. Lam, L.; Soong, R.; Sutrisno, A.; de Visser, R.; Simpson, M. J.; Wheeler, H. L.; Campbell, M.; Maas, W. E.; Fey, M.; Gorissen, A.; Hutchins, H.; Andrew, B.; Struppe, J.; Krishnamurthy, S.; Kumar, R.; Monette, M.; Stronks, H. J.; Hume, A.; Simpson, A. J. Comprehensive Multiphase NMR Spectroscopy of Intact 13C-Labeled Seeds, *J. Agric. Food Chem.* **2014**, *62*, 107-115.
- 52. Fortier-McGill, B.; Lam, L.; Soong, R.; Liaghati Mobarhan, Y.; Sutrisno, A.; de Visser, R.; Simpson, M. J.; Wheeler, H. L.; Campbell, M.; Gorissen, A.; Simpson, A. J. Comprehensive multiphase (CMP) NMR monitoring of the structural and molecular flux within a growing seed, *J. Agr. Food Chem.* **2017**, *65*, 6779-6788.
- 53. Wheeler, H. L.; Soong, R.; Courtier-Murias, D.; Botana, A.; Fortier-McGill, B.; Maas, W. E.; Fey, M.; Hutchins, H.; Krishnamurthy, S.; Kumar, R.; Monette, M.; Stronks, H. J.; Campbell, M. M.; Simpson, A. J. Comprehensive multiphase NMR: a promising technology to study plants in their native state, *Magn. Reson. Chem.* **2015**, *53*, 735-744.
- 54. Ghosh Biswas, R.; Fortier-McGill, B.; Akhter, M.; Soong, R.; Ning, P.; Bastawrous, M.; Jenne, A.; Schmidig, D.; De Castro, P.; Graf, S.; Kuehn, T.; Busse, F.; Struppe, J.; Fey, M.; Heumann, H.; Boenisch, H.; Gundy, M.; Simpson, M. J.; Simpson, A. J. Ex vivo Comprehensive Multiphase NMR of whole organisms: A complementary tool to in vivo NMR, *Anal. Chim. Acta* **2020**, *6*, 100051.
- 55. Liaghati Mobarhan, Y.; Soong, R.; Lane, D.; Simpson, A. J. In vivo comprehensive multiphase NMR, *Magn. Reson. Chem.* **2020**, *58*, 427-444.
- 56. Liaghati Mobarhan, Y.; Fortier-McGill, B.; Soong, R.; Maas, W. E.; Fey, M.; Monette, M.; Stronks, H. J.; Schmidt, S.; Heumann, H.; Norwood, W.; Simpson, A. J. Comprehensive multiphase NMR applied to a living organism, *Chem. Sci.* **2016**, *7*, 4856.
- 57. Ning, P.; Lane, D.; Ghosh Biswas, R.; Soong, R.; Schmidig, D.; Frei, T.; De Castro, P.; Kovacevic, I.; Graf, S.; Wegner, S.; Busse, F.; Kuehn, T.; Struppe, J.; Fey, M.; Stronks, H. J.; Monette, M.; Simpson, M. J.; Simpson, A. J. Comprehensive Multiphase NMR Probehead with Reduced Radiofrequency Heating Improves the Analysis of Living Organisms and Heat-Sensitive Sample, *Anal. Chem.* **2021**, 93, 10326-10333.
- 58. Ning, P.; Lane, D.; Soong, R.; Schmidig, D.; Frei, T.; De Castro, P.; Kovacevic, I.; Graf, S.; Wegner, S.; Busse, F.; Struppe, J.; Fey, M.; Stronks, H.; Monette, M.; Simpson, M. J.; Simpson, A. J. Comprehensive Multiphase NMR—A Powerful Tool to Understand and Monitor Molecular Processes during Biofuel Production, *ACS Sustainable Chem. Eng.* **2020**, *8*, 17551-17564.
- 59. Silva, L. M. A.; Filho, E. G. A.; Simpson, A. J.; Monteiro, M. R.; Venâncio, T. Comprehensive multiphase NMR spectroscopy: A new analytical method to study the effect of biodiesel blends on the structure of commercial rubbers, *Fuel*, **2016**, *166*, 436-445.
- 60. Hu, J. Z.; Sears, J. A.; Mehta, H. S.; Ford, J. J.; Kwak, J. H.; Zhu, K.; Wang, Y.; Liu, J.; Hoyt, D. W.; Peden, C. H. F. A large sample volume magic angle spinning nuclear magnetic resonance probe for *in situ* investigations with constant flow of reactants, *Phys. Chem. Chem. Phys.* **2011**, *14*, 2137-2143.

- 61. Antzutkin, O. N. Sideband manipulation in magic-angle-spinning nuclear magnetic resonance, *Prog. Nucl. Mag. Res. Sp.* **1999**, *35*, 203-266.
- 62. Song, Z.; Antzutkin, O. N.; Feng, X.; Levitt, M. H. Sideband suppression in magic-angle-spinning NMR by a sequence of 5  $\pi$  pulses, *Solid State Nucl. Mag.* **1993**, 2, 143-146.
- 63. Aguilar, J. A.; Nilsson, M.; Bodenhausen, G.; Morris, G. A. Spin echo NMR spectra without J modulation, *Chem. Commun.* **2012**, *48*, 811-813.
- 64. Jost, W. Diffusion in Solids, Liquids, Gases; Academic Press, New York, 1960.
- 65. Zhang, Y.; Xu, H.; Parsons, A. M.; Casabianca, L. B. Examining Binding to Nanoparticle Surfaces Using Saturation Transfer Difference (STD)-NMR Spectroscopy, *J. Phys. Chem. C* **2017**, *121*, 24678-24686.
- 66. Ghosh Biswas, R.; Soong, R.; Ning, P.; Lane, D.; Bastawrous, M.; Jenne, A.; Schmidig, D.; de Castro, P.; Graf, S.; Kuehn, T.; Kümmerle, R.; Bermel, W.; Busse, F.; Struppe, J.; Simpson, M. J.; Simpson, A. J. Exploring the Applications of Carbon-Detected NMR in Living and Dead Organisms Using a 13C-Optimized Comprehensive Multiphase NMR Probe, *Anal. Chem.* **2022**, *94*, 8756-8765.

# Table of contents graphic:

